Molecular Staging of Cervical Lymph Nodes in Squamous Cell Carcinoma of the Head and Neck

Robert L. Ferris,[1,2] Liqiang Xi,[2,3] Siva Raja,[3] Jennifer L. Hunt,[4] Jun Wang,[1,2] William E. Gooding,[2,5] Lori Kelly,[2] Jesus Ching,[6] James D. Luketich,[2,3] and Tony E. Godfrey[2,3]

[1]Departments of Otolaryngology and Immunology, [2]University of Pittsburgh Cancer Institute, Departments of [3]Surgery, [4]Pathology, and [5]Biostatistics, University of Pittsburgh, Pittsburgh, Pennsylvania; and [6]Cepheid, Sunnyvale, California

Abstract

Clinical staging of cervical lymph nodes from patients with squamous cell carcinoma of the head and neck (SCCHN) has only 50% accuracy compared with definitive pathologic assessment. Consequently, both clinically positive and clinically negative patients frequently undergo neck dissections that may not be necessary. To address this potential overtreatment, sentinel lymph node (SLN) biopsy is currently being evaluated to provide better staging of the neck. However, to fully realize the potential improvement in patient care afforded by the SLN procedure, a rapid and accurate SLN analysis is necessary. We used quantitative reverse transcription–PCR (QRT-PCR) to screen 40 potential markers for their ability to detect SCCHN metastases to cervical lymph nodes. Seven markers were identified with good characteristics for identifying metastatic disease, and these were validated using a set of 26 primary tumors, 19 histologically positive lymph nodes, and 21 benign nodes from patients without cancer. Four markers discriminated between positive and benign nodes with accuracy >97% but only one marker, pemphigus vulgaris antigen (PVA), discriminated with 100% accuracy in both the observed data and a statistical bootstrap analysis. A rapid QRT-PCR assay for PVA was then developed and incorporated into a prototype instrument capable of performing fully automated RNA isolation and QRT-PCR. The automated analysis with PVA provided perfect discrimination between histologically positive and benign lymph nodes and correctly identified two lymph nodes with micrometastatic tumor deposits. These assays were completed (from tissue to result) in ~30 minutes, thus demonstrating the feasibility of intraoperative staging of SCCHN SLNs by QRT-PCR. (Cancer Res 2005; 65(6): 2147-56)

Introduction

Squamous cell carcinoma of the head and neck (SCCHN) frequently metastasizes to the regional lymph nodes and this is the strongest predictor of disease prognosis and outcome (1, 2). Whereas accurate staging of lymph nodes in the neck is essential for optimal patient management, current preoperative clinical methods, including newer radiographic techniques, are suboptimal and misdiagnose the presence or absence of cervical nodal metastasis in many patients (3–5). Therefore, due to the low sensitivity of detecting nodal metastasis and the poor prognosis when these metastases are missed, the current management of the clinically node negative (cN0) neck commonly includes routine elective neck dissection (END) with pathologic examination of the removed lymph nodes.

END, or cervical lymphadenectomy done at the time of primary surgery for SCCHN for a cN0 neck, is associated with a significantly improved regional recurrence-free survival and lower incidence of distant metastases (6–9). Furthermore, when END is not done, patients often present later with bulky neck metastases and unresectable disease. END not only provides more accurate staging, it also provides objective criteria to decide when to give adjuvant therapies, such as number/levels of cervical lymph nodes involved and the presence of extracapsular spread of tumor. However, upon END and pathologic analysis of neck dissections, only 25% to 30% of clinically negative necks are found to harbor pathologic evidence of disease (10–12), and 15% of clinically positive necks are in fact tumor negative (6, 13). Consequently, lymphadenectomy may represent overtreatment of almost 50% of patients. Even with END, 7% to 15% of patients with no pathologic evidence of cervical lymph node metastases (pN0) will nonetheless suffer disease recurrence in the neck, indicating the limitation of routine pathology for identifying micrometastasis (13–16).

Because of the need to accurately stage the neck and to treat only those most likely to benefit from therapy, much interest has arisen recently to validate the technique of sentinel lymph node (SLN) mapping for SCCHN. This technique has the *potential* to define those cN0 patients in whom neck dissection is most appropriate (i.e., those who are pathologically node positive), thereby obviating END and its associated morbidities in node-negative patients. Numerous single-institution studies have suggested that SLN mapping in SCCHN accurately predicts the status of the neck (5, 17–21), and this finding is currently being evaluated in a large multicenter validation trial sponsored by the American College of Surgeons Oncology Group (ACOSOG Z0360 trial). When combined with intraoperative analysis of the SLN(s), this approach could allow for definitive staging and surgical treatment in a single procedure. For this goal to be fully realized, however, intraoperative SLN analysis must be both rapid and accurate.

Unfortunately, although final pathology on fixed tissues (with immunostaining if necessary in the case of SLNs) is highly accurate, intraoperative frozen section examination is notoriously insensitive. In breast cancer, reports on intraoperative SLN sensitivity range from 47% to 74% (22, 23) whereas in melanoma the sensitivity is even worse, with reports from 38% to 47% (24, 25). Consequently, many patients have to undergo a second surgical

Note: R.L. Ferris and L. Xi contributed equally to this work.

L. Xi and T.E. Godfrey are currently at Mount Sinai School of Medicine, New York, New York.

Supplementary data for this article are available at Cancer Research Online (http://cancerres.aacrjournals.org/) and at http://www.mssm.edu/labs/godfrt01/publications/supp.htm.

Requests for reprints: Tony E. Godfrey, Mount Sinai School of Medicine, Box 1079, One Gustave L. Levy Place, New York, NY 10029. Phone: 212-659-9082; Fax: 212-828-4221; E-mail: tony.godfrey@mssm.edu or Robert L. Ferris, University of Pittsburgh Cancer Institute, Hillman Research Wing 1.19d, 5117 Centre Avenue, Pittsburgh, PA 15213. Phone: 412-623-7703; E-mail: ferrisrl@upmc.edu.

procedure to complete lymph node dissection after definitive pathologic assessment identifies microscopic metastatic disease not evident on intraoperative analysis. Our own work, and that reported by others, suggests that low sensitivity may also be an issue for intraoperative SLN analysis in SCCHN (18, 21). Performing a second surgery on the neck is an undesirable scenario because this would likely increase complications and morbidity and could delay the use of adjuvant therapy. This is in addition to the extra cost, discomfort, and psychological toll on the patient. Such issues may negatively affect the widespread acceptance of SLN biopsy in SCCHN.

Reverse transcription–PCR (RT-PCR) has great theoretical potential for the detection of small tumor deposits in lymph nodes. Studies in many tumor types including esophageal cancer, colon cancer, breast cancer, melanoma, and SCCHN have showed the ability of an RT-PCR–based assay to detect histologically occult micrometastases (7, 9, 26–29). Many of the earlier RT-PCR studies suffered from poor specificity, but the introduction of real-time quantitative RT-PCR (QRT-PCR) has helped overcome this problem and provides the potential for objective and quantitative analysis of lymph nodes (30–33). Whereas we are also interested in detection of occult disease by QRT-PCR, we have recently focused on application of this method to rapid, intraoperative analysis of SLNs. We have shown that RNA isolation and QRT-PCR can be done in a time frame amenable to intraoperative analysis and we have also developed multiplex PCR technology to allow incorporation of necessary controls into rapid QRT-PCR (34, 35). Unfortunately, these reports used manual RNA isolation and QRT-PCR setup, and this is likely to be too labor intensive, prone to contamination, and variable for true clinical use in an intraoperative setting. This concern has recently been addressed, however, with the development of a fully automated and integrated RNA isolation and quantitative PCR instrument called the GeneXpert (Cepheid, Sunnyvale, CA).[7] The GeneXpert is capable of performing RNA isolation from lysed tissue, reverse transcription, and quantitative PCR all in ~30 minutes. Our goals in this study were to identify appropriate QRT-PCR markers for detection of metastasis to lymph nodes and to use the GeneXpert to show the feasibility of automated analysis in an intraoperative time frame. When applied to SLNs from patients with SCCHN, we show that this technology has the potential to accurately stage the neck and allow the surgeon to provide optimal treatment in a single procedure.

Materials and Methods

Patients

A total of 26 primary tumors and 24 histologically tumor involved nodes were harvested at surgery and immediately snap-frozen at −80°C until RNA extraction was done. Of these specimens, eight sets of paired human head and neck primary tumors and tumor-containing metastatic lymph nodes (from the same 8 patients with SCCHN) were included in this study. Benign lymph nodes (n = 21) were obtained from patients undergoing surgery for benign esophageal disorders (gastroesophageal reflux or achalasia). Institutional review board–approved, written informed consent was obtained from all patients donating specimens for this study, either through the ENT Registry at the Department of Otolaryngology or the Esophageal Risk Registry at the Division of Thoracic and Foregut Surgery, University of Pittsburgh. Clinical and demographic data for fresh tumor/metastasis specimens are shown in Table 1. These patients are similar to historical patients with SCCHN in our practice, with tumors distributed throughout all head and neck subsites. In the 44 patients studied, histologically verified squamous cell carcinoma originated in one of the following primary sites: oral cavity (18), oropharynx (10), larynx (10), hypopharynx (5), and site undetermined (1).

Identification of Potential Markers

An extensive literature and public database survey was conducted to identify any potential markers. Resources for this survey included PubMed, OMIM, UniGene (http://www.ncbi.nlm.nih.gov/), GeneCards (http://bioinfo.weizmann.ac.il/cards), and CGAP (http://cgap.nci.nih.gov). Our survey criteria were somewhat flexible but the goal was to identify genes with moderate to high expression in head and neck cancer and low expression in normal lymph nodes. In addition, genes reported to be up-regulated in head and neck cancer and genes with restricted tissue distribution were considered potentially useful. Finally, genes reported to be cancer specific, such as the cancer testis antigens and *hTERT*, were evaluated.

Tissues and Pathologic Evaluation

Archived tissue from all patients in this study was reviewed by a specialized head and neck pathologist (J.L.H.), and the diagnosis was reconfirmed histologically. Twenty 5-μm sections were cut from each optimal cutting temperature compound (OCT)–embedded tissue for RNA isolation. In addition, sections were cut and placed on slides for H&E and immunohistochemistry analysis at the beginning, middle (between the 10th and 11th sections for RNA), and end of the sections for RNA isolation. All three H&E slides from each specimen underwent pathologic review to confirm presence of tumor, percentage of tumor, and to identify the presence of any contaminating tissues. All of the unstained slides were stored at −20°. Immunohistochemistry evaluation was done using the antibody pan keratin (AE1/AE3) mixture (DAKO, Carpinteria, CA), and Vector Elite ABC kit and Vector AEC Chromagen (Vector Laboratories, Burlingame, CA). Immunohistochemistry was used as needed to confirm the H&E histology.

Screening Approach

The screening was conducted in two phases. All potential markers entered the primary screening phase and expression was analyzed in 6 primary tumors and 10 benign lymph nodes obtained from patients without cancer (five RNA pools with 2 lymph node RNAs per pool). Markers that showed good characteristics for lymph node metastasis detection (consistent, high expression in tumors and very low expression in benign nodes) passed into the secondary screening phase. The secondary screen consisted of expression analysis on 26 primary tumors, 19 histologically positive lymph nodes, and 21 benign lymph nodes without cancer.

RNA Isolation and cDNA Synthesis

RNA was isolated using the RNeasy minikit (Qiagen, Valencia, CA) essentially as described by the manufacturer. The only modification was that we doubled the volume of lysis reagent and loaded the column in two steps. This was found to provide better RNA yield and purity, probably because of diluting out the OCT in the tissue sections. Reverse transcription was done in 100-μL reaction volumes with random hexamer priming and SuperScript II (Invitrogen, Carlsbad, CA) reverse transcriptase (36). For the primary screen, two reverse transcription reactions were done, each with 1,000 ng of RNA. The cDNAs were combined and quantitative PCR was done using the equivalent of 20 ng RNA per reaction. For the secondary screen, the RNA input for primary tumors and positive nodes was 1200 ng per reverse transcription reaction and 20 ng per quantitative PCR reaction, but this was increased to 2000 ng per reverse transcription reaction and 80 ng per quantitative PCR reaction for the benign nodes in order to improve sensitivity for detection of low background expression.

Quantitative PCR

All quantitative PCR for marker screening was done on the ABI Prism 7700 Sequence Detection Instrument (Applied Biosystems, Foster City, CA). Relative expression of the marker genes was calculated using the ΔC_T methods previously described (37) and with β-glucuronidase as

[7] Manuscript submitted for publication.

Table 1. Clinical and demographic data of tumor and lymph node specimens obtained from patients with SCCHN in this study

Patient no.	Age (y)	Gender	Primary site	Stage	Grade of differentiation	Specimen given	% Tumor
1	65	Male	Tongue	T1N0M0	Moderate	Primary	4
2	50	Male	Tongue	T3N1M0	Moderate	Primary	5
3	67	Male	Larynx	T2N0M0	Moderate	Primary	7.5
4	60	Female	Tongue	T2N0M0	Moderate	Primary	10
5	53	Female	Oropharynx	T1N2M0	Moderate	Primary	12.5
6	70	Male	Oral cavity	T2N1M0	Moderate	Primary	15
7	50	Male	Larynx	T1N0M0	Moderate	Primary	15
8	74	Female	Larynx	T3N0M0	Moderate	Primary	15
9	70	Female	Oral cavity	T4N1M0	Moderate	Primary	20
10	62	Male	Larynx	T4N2M0	Moderate	Primary	25
11	65	Female	Oral cavity	T4N0M0	Moderate	Primary	30
12	56	Male	Larynx	T3N3M0	Moderate	Primary	35
13	49	Male	Oral cavity	T2N0M0	Moderate	Primary	35
14	59	Male	Oropharynx	T2N0M0	Poor	Primary	35
15	59	Male	Oropharynx	T2N0M0	Poor	Primary	40
16	57	Male	Oral cavity	T4N1M0	Moderate	Primary	50
17	64	Female	Oropharynx	T1N0M0	Poor	Primary	50
18	71	Male	Oropharynx	T3N0M0	Poor	Primary	65
19	74	Male	Larynx	T3N2M0	Moderate	Primary	65
						Positive node	40
20	76	Male	Hypopharynx	T4N2cM0	Moderate	Primary	77.5
						Positive node	40
21	51	Male	Oropharynx	T2N2cM0	Moderate	Primary	40
						Positive node	50
22	49	Male	Oropharynx	T3N3M0	Poor	Primary	40
						Positive node	60
23	76	Male	Oropharynx	T2N2M0	Poor	Primary	50
						Positive node	75
24	48	Male	Larynx	T3N2cM0	Poor	Primary	50
						Positive node	40
25	50	Male	Oral cavity	T4N2bM0	Well	Primary	60
						Positive node	90
26	51	Male	Oral cavity	T4N1M0	Moderate	Primary	60
						Positive node	40
27	69	Male	Larynx	T4N3M0	Poor	Positive node	70
28	66	Female	Larynx	T3N2cM0	Poor	Positive node	80
29	43	Male	Oropharynx	T1N2bM0	Poor	Positive node	90
30	78	Male	Buccal	T2N2	Moderate	Positive node	90
31	53	Male	Tonsil	T2N2a	Moderate	Positive node	5
32	54	Female	Oral cavity	T2N1	Poor	Positive node	30
33	71	Male	Oral cavity	T4N0	Poor	Positive node	30
34	56	Male	Hypopharynx	T1N2b	Moderate	Positive node	40
35	79	Male	Hypopharynx	T2N2c	Moderate	Positive node	40
36	65	Male	Unknown	T4N2c	Moderate	Positive node	40
37	67	Male	Tongue	T3N2c	Poor	Positive node	60
38	65	Male	Tongue	T2N1	Moderate	Positive node	<1
39	45	Female	Tongue	T2N2b	Poor	Positive node	20
40	72	Female	Hypopharynx	T1N2	Moderate	Positive node	90
41	54	Female	Hypopharynx	T3N2b	Moderate	Positive node	60
42	67	Male	Tongue	T3N2	Moderate	Positive node	10
43	68	Female	Tongue	T2N1	Poor	Positive node	25
44	44	Male	Oral cavity	T1N2b	Poor	Positive node	<1

the endogenous control gene. All assays were designed for use with 5′ nuclease hybridization probes although the primary screening was done using SYBR Green quantification to save cost. Assays were designed using the ABI Primer Express Version 2.0 software and, where possible, amplicons spanned exon junctions in order to provide cDNA specificity. All primer pairs were tested for amplification specificity (generation of a single band on gels) at 60°C, 62°C, and 64°C annealing temperature. In addition, PCR efficiency was estimated using SYBR Green quantification before use in the primary screen. Further optimization and more precise estimates of efficiency were done with 5′ nuclease probes for all assays used in the secondary screen.

A mixture of the Universal Human Reference RNA (Stratagene, La Jolla, CA) and RNAs from human placenta, thyroid, heart, colon, PCI13 cell line (gift of Dr. Theresa Whiteside, University of Pittsburgh Cancer Institute) and SKBR3 cell line served as a universal positive expression control for all the genes in the marker screening process.

Quantification with SYBR Green (Primary Screen)

For SYBR Green I–based quantitative PCR, each 50-μL reaction contained 1× TaqMan buffer A (Applied Biosystems), 300 nmol/L each deoxynucleotide triphosphate, 3.5 mmol/L $MgCl_2$, 0.06 units/μL Amplitaq Gold (Applied Biosystems), 0.25× SYBR Green I (Molecular Probes, Eugene, OR), and 200 nmol/L each primer. The amplification program consisted of two stages with an initial 95°C Taq activation stage for 12 minutes followed by 40 cycles of 95°C denaturation for 15 seconds, 60°C, 62°C, or 64°C anneal/extend for 60 seconds, and a 10-second data collection step at a temperature 2°C to 4°C below the T_m of the specific PCR product being amplified (38). After amplification, a melting curve analysis was done by collecting fluorescence data while increasing the temperature from 60°C to 95°C over 20 minutes.

Quantification with 5′ Nuclease Probes (Secondary Screen)

Probe-based quantitative PCR was done as described previously (26, 37). Briefly, reactions were done with a probe concentration of 200 nmol/L and a 60-second anneal/extend phase at 60°C for *β-GUS*, *CK19*, *PTHrP*, and *SCCA1/2*, 62°C for pemphigus vulgaris antigen (*PVA*), and 64°C for carcinoembryonic antigen (*CEA*) and *TACSTD1*. The sequences of primers and probes (purchased from IDT, Coralville, IA) for genes evaluated in the secondary screen are listed in Supplementary Table 1. The primer sequences for markers used in the primary screen will be provided upon request.

Data Analysis

In the primary screen, data from the melting curve were analyzed using the ABI Prism 7700 Dissociation Curve Analysis 1.0 software (Applied Biosystems). The first derivative of the melting cure was used to determine the product T_m as well as to establish the presence of the specific product in each sample. In general, samples were analyzed in duplicate PCR reactions and the average C_t value was used in the expression analysis. However, in the secondary screen triplicate runs were done for each individual benign node and the lowest C_t value was used in the calculation of relative expression to obtain the highest value of background expression for the sample.

Statistical Analysis

Generation of Prediction Rules. Six markers that passed the secondary screen were evaluated individually and in combination with other markers. The characteristics used to evaluate markers were sensitivity, specificity, classification, accuracy and the area under the receiver operating characteristic curve. For individual markers, a cutoff value was determined that maximized the classification accuracy (proportion of lymph nodes correctly classified). In cases wherein classification accuracy was 100%, the cutoff was set at the midpoint between the highest expressing negative node and the lowest expressing positive node. Markers were also combined into pairs for lymph node classification and a linear prediction rule was generated for each pair. The rule was equivalent to the linear predictor that equalized the fitted probabilities above and below the linear boundary. That is, points on the boundary line had a predicted probability midway between the numerical scores assigned to positive and negative nodes. For example, if positive nodes were assigned a score of 2 and benign nodes a score of 1, predicted scores >1.5 were classified as positive.

Internal Validation of Prediction Rules. Internal validation of prediction rules was conducted by nonparametric bootstrap resampling using Efron and Tibshirani's improved bootstrap method (39), in which 500 bootstrap samples of lymph nodes are selected from the pool of all positive and negative nodes. The optimism in the original estimates of sensitivity, specificity, and classification accuracy are then calculated as the difference between the bootstrap classification statistic applied to the original data and applied to the bootstrap data. The average difference over all bootstrap samples is computed and reported as the bias in the values derived from the observed data and then subtracted from the original estimates to produce the bootstrap-validated estimates.

GeneXpert Analysis. Twenty-four 5-μm sections of OCT-embedded tissue were sectioned into 800 μL of GeneXpert lysis buffer (Cepheid). The lysis buffer was filtered through a 0.22-mm syringe filter (Osmonics Inc, Westborough, MA), and loaded into a GeneXpert cartridge. The automated processes of RNA isolation, reverse transcription, and QRT-PCR on the GeneXpert are described elsewhere.[7] Briefly, the filtered tissue lysate is placed into a reservoir on the GeneXpert cartridge (Supplemental Fig. 1, panel 5) and all necessary reagents for RNA isolation, reverse transcription and quantitative PCR are placed in additional reservoirs. The cartridge is placed in the GeneXpert (Supplemental Fig. 1, panel 6) and the remaining steps are fully automated. The tissue lysate is first passed over an RNA isolation resin, washed, and then RNA is eluted into a clean reservoir (~6 minutes). Reverse transcription reagents are added and the mixture is pumped into the integrated PCR tube and heated for cDNA synthesis (~5 minutes). The cDNA is then removed from the PCR tube and PCR reagents (primers, probes, etc.) are added. The mixture is returned to the PCR tube and thermal cycling is done (~20-25 minutes). Probe fluorescence is monitored at each cycle and results are updated on the monitor in real time. For this study, the PCR assay consisted of a multiplex QRT-PCR for PVA and the endogenous control gene, β-glucuronidase. This assay was optimized to perform in a rapid, multiplex PCR protocol using our previously published methods for rapid PCR and temperature-controlled primer limiting (34, 35).

Results

Primary Screening. Our literature and database surveys identified 40 genes for evaluation in the primary tumor marker screen. All of these genes were analyzed for expression in 6 primary SCCHN and 10 benign lymph nodes. Resulting data for the 20 genes with the highest median expression in tumors is shown in Fig. 1 and similar data for all genes in the primary screen will be provided upon request. Histograms showing the data from all genes in the primary screen can also be viewed at http://www.mssm.edu/labs/godfrt01/research/charts.htm. Median relative expression in the

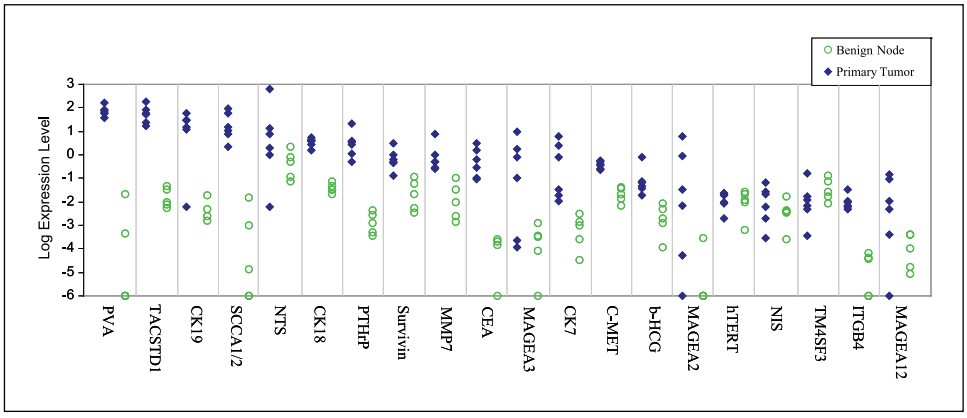

Figure 1. Primary screen data showing the expression profiles of top 20 genes ranked by median expression in 6 primary head and neck tumors and 10 benign lymph nodes from the patients without cancer.

Table 2. Relative expression in head and neck tumors and benign lymph nodes for the markers analyzed in the primary screen

Gene	Accession number	Median tumor	Median benign node	Highest benign node	Lowest tumor/highest benign node	Median tumor/ highest benign node
PVA	NM_001944	67.476213	—*	0.021197	1770.6	3183.3
TACSTD1	NM_002354	56.962817	0.009753	0.049549	339.0	1149.6
CK19	NM_002276	22.922226	0.003691	0.018136	0.3	1263.9
SCCA1/2†	NM_006919	13.372098	0.000014	0.015571	147.0	858.8
NTS	NM_006183	4.880276	0.532185	2.321408	0.003	2.1
CK18	NM_000224	3.890994	0.033609	0.073557	22.1	52.9
PTHrP	NM_002820	3.175056	0.001186	0.004425	117.8	717.5
Survivin	NM_001169	0.570393	0.022251	0.113834	1.2	5.0
MMP7	NM_002423	0.506164	0.009453	0.099098	2.5	5.1
CEA	NM_004363	0.467097	0.000175	0.000270	340.1	1730.3
MAGEA3	NM_005362	0.457354	0.000328	0.001271	0.1	359.9
CK7	NM_005556	0.435114	0.000953	0.003162	3.2	137.6
C-MET	NM_000245	0.385698	0.020617	0.039692	5.9	9.7
bHCG	NM_000737	0.058275	0.001893	0.009005	2.0	6.5
MAGEA2	NM_005361	0.019915	—*	0.000279	—‡	71.3
hTERT	NM_003219	0.014411	0.012648	0.026645	0.1	0.5
NIS	NM_000453	0.014012	0.003933	0.016232	0.02	0.9
TM4SF3	NM_004616	0.009610	0.025295	0.136787	0.003	0.1
ITGB4	NM_000213	0.008011	0.000038	0.000063	74.8	126.3
MAGEA12	NM_005367	0.007785	0.000103	0.000404	—‡	19.3
CK14	NM_000526	0.007772	—§	—§	∞	∞
LDHC	NM_017448	0.006556	—*	0.016402	—‡	0.4
MAGEA1	NM_004988	0.003538	—§	—§	—‡	∞
BRDT	NM_001726	0.002530	0.000278	0.000350	—‡	7.2
STX	NM_006011	0.001549	0.000030	0.000194	4.2	8.0
TITF1	NM_003317	0.001444	0.001320	0.007625	0.1	0.2
Villin1	NM_007127	0.000839	0.000288	0.000433	0.5	1.9
MAGEA10	NM_021048	0.000816	—§	—§	—‡	∞
MAGEA8	NM_005364	0.000675	—§	—§	—‡	∞
KRTHB1	NM_002281	0.000570	—*	0.000165	—‡	3.5
CK20	NM_019010	0.000324	—§	—§	—‡	∞
SGY-1	NM_014419	0.000305	0.000134	0.000605	—‡	0.5
CTAG1	NM_001327	0.000206	—*	0.002036	—‡	0.1
SSX2	NM_003147	0.000153	—§	—§	—‡	∞
GAGE1	NM_001468	0.000060	—*	0.000703	—‡	0.1
GAGEu†		—§	—*	0.000126	—‡	—‡
BAGE	NM_001187	—§	—*	0.000152	—‡	—‡
CDX1	NM_001804	—§	—*	0.000016	—‡	—‡
MAGEA4	NM_002362	—§	—§	—§	—‡	—‡
SSXu‡		—§	—§	—§	—‡	—‡

Note: Data are ranked by median expression in tumors. ∞, no detectable expression in benign nodes.
*Three or more samples were at nondetectable level in 40-cycle quantitative PCR.
†Universal design to amplify all members in the gene family.
‡Lowest or median expression level of tumor was at nondetectable level in 40-cycle quantitative PCR.
§All samples tested were at non-detectable level in 40 cycle qPCR.

primary tumors and benign nodes was calculated for each gene in the primary screen and is reported in Table 2. In addition, we also calculated the ratio of relative expression between the lowest expressing tumor and the highest expressing benign node, and between the median expression in tumors and the highest expressing benign node. Some genes had no detectable expression in benign nodes and therefore ratios could not be calculated (see Table 2).

Using these three parameters (median expression in the tumors, lowest tumor/highest benign node and median tumor/highest benign node ratios), we selected six genes that we judged to have expression characteristics suitable for detection of lymph node metastases. These six genes, *PVA*, *CEA*, *CK19*, *PTHrP*, *SCCA1/2*, and *TACSTD1*, all have median tumor/highest benign node ratios >500 and therefore have the potential to detect small foci of tumor while still discriminating negative nodes. In addition, all genes except *CK19* also have lowest tumor/highest benign node ratios >100 indicating that they are expressed at reasonably high levels in all six tumors tested in the primary screen. *MAGEA3* and *CK7* were omitted from the secondary

screen due to a combination of low median tumor/highest benign node expression ratios and relatively low median expression in tumors. Similarly, *CK18* was excluded based on a combination of low expression ratios and *ITGB4* was excluded due to very low median expression in primary tumors. Finally, *EGFR* was inadvertently omitted from the primary screen but was included in the secondary screen based on its frequent use as a marker in SCCHN studies (40–42).

Secondary Screen. Histologic evaluation of the 26 primary tumor specimens revealed a median tumor percentage of 40% (range, 5-95%). Similarly, in the 19 histologically positive nodes, the median tumor percentage was 70% (range, 2-90%). The relative expression profiles of the markers selected for the secondary screen are shown in Fig. 2*A*. The data shows that all markers are expressed in positive lymph nodes as well as in primary tumors indicating that metastatic tumor cells continue to express these genes. Figure 2*A* also indicates the relative expression cutoff values that provide the most accurate classification of histologically positive and benign nodes. These cutoff values were used to calculate classification characteristics (sensitivity, specificity, area under the receiver operating curve, and overall classification accuracy) for each marker and the results are presented in Table 3.

Of the seven markers analyzed, two (*PVA* and *SCCA1/2*) provided perfect classification of positive and benign lymph nodes. *PTHrP* and *TACSTD1* also proved to be very good markers, with classification accuracy of 97.5%. The remaining three markers, however, suffered from poor sensitivity (*EGFR* and *CK19*) or poor specificity (*CEA* and *CK19*), resulting in overall classification accuracy of 95% or less. For all markers, these estimates of classification accuracy are likely to be optimistic because the cutoff value is being generated and tested on the same data set. In an attempt to address this issue, we did an internal marker validation using nonparametric bootstrap analysis to estimate the optimism in our observed classification accuracy. The results, shown in Table 3, indicate that *PVA* is the only marker that retained 100% accuracy in the bootstrap analysis. For *SCCA1/2*, *PTHrP*, and *TACSTD1* the bias, or estimate of optimism in the observed data, was ≤1.3% and these genes are likely to provide classification accuracy >96% if tested in a larger sample set. The bias for *CEA*, *CK19*, and *EGFR*, on the other hand, ranged from 2.2% to 7.8%, and the estimates of true classification accuracy were all <93%. Thus, it seems that *PVA* is the single best marker identified in this study, with *SCCA1/2*, *PTHrP*, and *TACSTD1* also being strong individual markers.

In addition to analyzing individual markers, we also evaluated lymph node classification using paired combinations of *PVA*, *SCCA1/2*, *PTHrP*, and *TACSTD1*. Marker pairs were evaluated by plotting graphs with expression of one marker on each of the

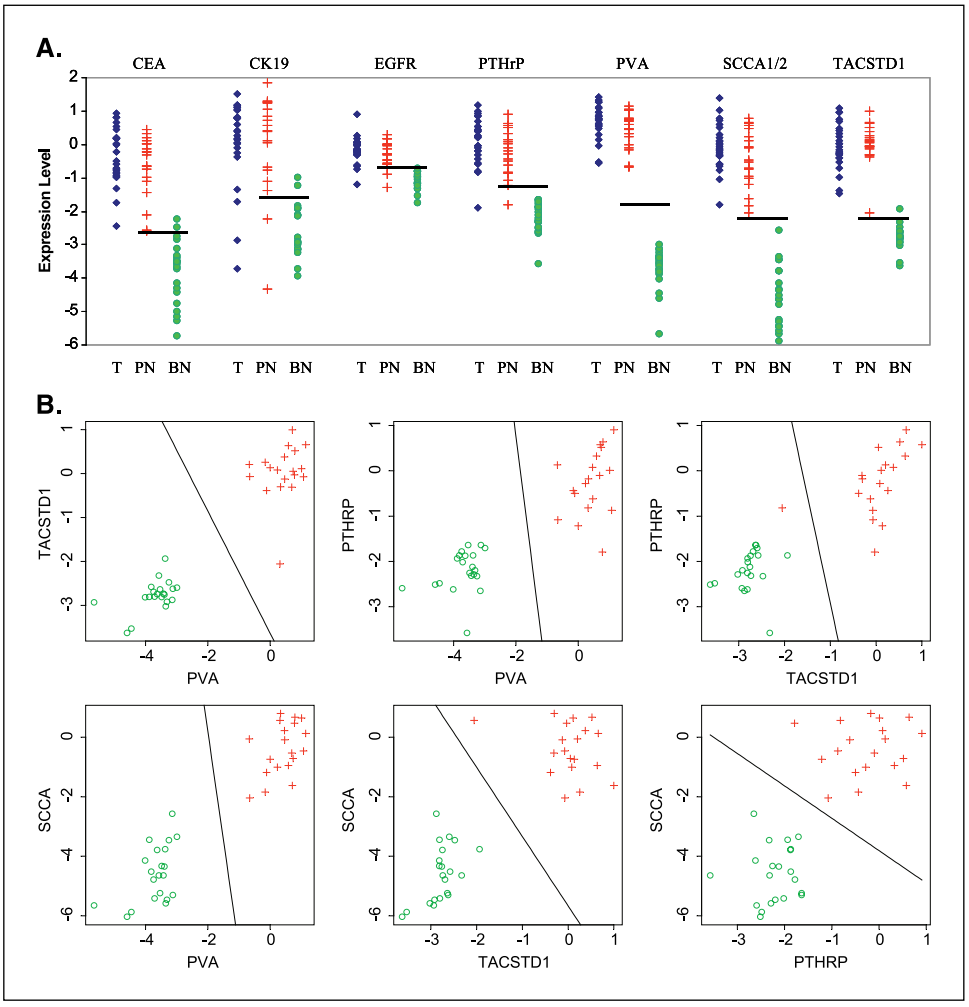

Figure 2. Secondary screen data: *A*, expression profiles of selected markers in primary head and neck tumors (*T*), histologically positive lymph nodes (*PN*), and benign lymph nodes (*BN*) from the patients without cancer. *B*, two marker prediction on histologically positive nodes (*red plus sign*) and benign lymph nodes (*green circle*).

Table 3. Single- or two-marker prediction characteristics on positive and benign lymph nodes in the secondary screen

Marker	Observed data			Parametric bootstrap estimates*			Classification bias†
	Sensitivity	Specificity	Classification accuracy	Sensitivity	Specificity	Classification accuracy	
CEA	1.0	0.905	0.950	0.974	0.880	0.872	0.078
CK19	0.895	0.905	0.900	0.867	0.880	0.872	0.028
EGFR	0.895	1.0	0.947	0.873	0.979	0.925	0.022
PTHrP	0.947	1.0	0.975	0.938	0.988	0.963	0.012
PVA	1.0	1.0	1.0	1.0	1.0	1.0	0.000
SCCA1/2	1.0	1.0	1.0	0.998	0.985	0.991	0.009
TACSTD1	1.0	0.952	0.975	0.983	0.944	0.962	0.013
PVA + TACSTD1	1.0	1.0	1.0	0.993	1.0	0.997	0.003
PVA + PTHrP	1.0	1.0	1.0	1.0	1.0	1.0	0.000
PVA + SCCA1/2	1.0	1.0	1.0	1.0	1.0	1.0	0.000
TACSTD1 + PTHrP	0.947	1.0	0.975	0.944	1.0	0.974	0.001
TACSTD1 + SCCA1/2	1.0	1.0	1.0	0.984	1.0	0.992	0.008
PTHrP + SCCA1/2	1.0	1.0	1.0	1.0	1.0	1.0	0.000

*Five hundred bootstrap samples of lymph node expression levels were generated and a new decision rule based on the most accurate cutoff was formulated each time (total of 500 decision rules). The optimism for each bootstrap sample is calculated as the difference between the classification statistics applied to the original data and applied to the bootstrap data. The average over all bootstrap samples is computed and reported as the bias in the values derived from the observed data (Efron's enhanced bootstrap prediction error estimate; see Efron B, Tibshirani RJ. An introduction to the bootstrap. Boca Raton: Chapman and Hall/CRC Press; 1993).

†Bias is the enhanced bootstrap estimate of optimism, or the amount that classification accuracy is overestimated when tested on the original data.

axes and then mathematically calculating a linear cutoff that was midway between the positive and negative lymph node distributions (Fig. 2*B*). Classification accuracy obtained for all marker combinations using this approach is shown in Table 3 (observed data) and all but one combination (*TACSTD1/PTHrP*) achieved an observed classification accuracy of 100%. As with the individual markers, this is likely to be optimistic, and nonparametric bootstrap analysis was therefore done. We found that classification accuracy dropped <0.8% compared with the observed data (Table 3, nonparametric bootstrap estimates) indicating that marker combinations are likely to provide more robust lymph node classification than single markers alone.

Automated Analysis of Lymph Nodes. To show the potential for rapid and automated QRT-PCR analysis of lymph nodes, we analyzed a set of seven benign and seven histologically positive lymph nodes for expression of *PVA* using the Cepheid GeneXpert instrument. As in the screening data, we found that *PVA* expression was almost 2 orders of magnitude higher in all positive nodes than in any benign node, and in most cases was >3 orders of magnitude higher. Interestingly, two lymph nodes in this set were called positive by final pathology (on the lymph node half that was sent for routine pathologic analysis with H&E staining of fixed tissue) but were apparently negative by H&E staining of the frozen sections adjacent to the sections used for RT-PCR analysis. Pan-keratin immunostaining of these sections, however, revealed extremely small foci of positively staining cells (Fig. 3*B*) and QRT-PCR for *PVA* on the GeneXpert also identified these nodes as positive (nodes 1957 and 2634 in Fig. 3). These micrometastases would likely have been missed on intraoperative frozen section analysis. Thus, *PVA* expression measured on the automated GeneXpert instrument clearly differentiated positive and benign nodes in this sample set and correctly identified two nodes with micrometastatic disease. In addition, all assays were done in 30 minutes or less, demonstrating the potential for intraoperative analysis of SLNs in head and neck cancer.

Discussion

Current analysis of lymph nodes with H&E staining and microscopic examination suffers from two major limitations. First, only one or two tissue sections are typically reviewed, leaving the majority of each node unsampled, and second, small foci of tumor cells can be missed. These limitations are even more pronounced for intraoperative frozen section analysis due to poor tissue architecture and time constraints. Whereas it has been shown that serial sectioning can overcome the issue of sampling error (43, 44) and that the addition of immunohistochemistry staining can improve detection of small tumor foci (28), the combination of these methods is too time-consuming for intraoperative lymph node analysis. Because cost is also an issue, this detailed analysis approach is limited to examination of fixed tissues in diseases in which SLN biopsy is done, thus reducing the number of lymph nodes to be examined. Unfortunately, permanent section results are not available until several days after lymphadenectomy and, therefore, for intraoperative decision making, the surgeon currently has to rely on frozen-section H&E analysis. In the treatment of breast cancer and melanoma, in which SLN biopsy is commonly used, the sensitivity of intraoperative frozen-section analysis ranges from 38% to 74% (22–25). Consequently, many patients have to undergo second surgeries to complete lymph node dissection, in cases in which definitive pathologic assessment identifies metastases that were missed on the frozen-section examination. The limited reports on frozen-section sensitivity in SCCHN suggest that a similar scenario is

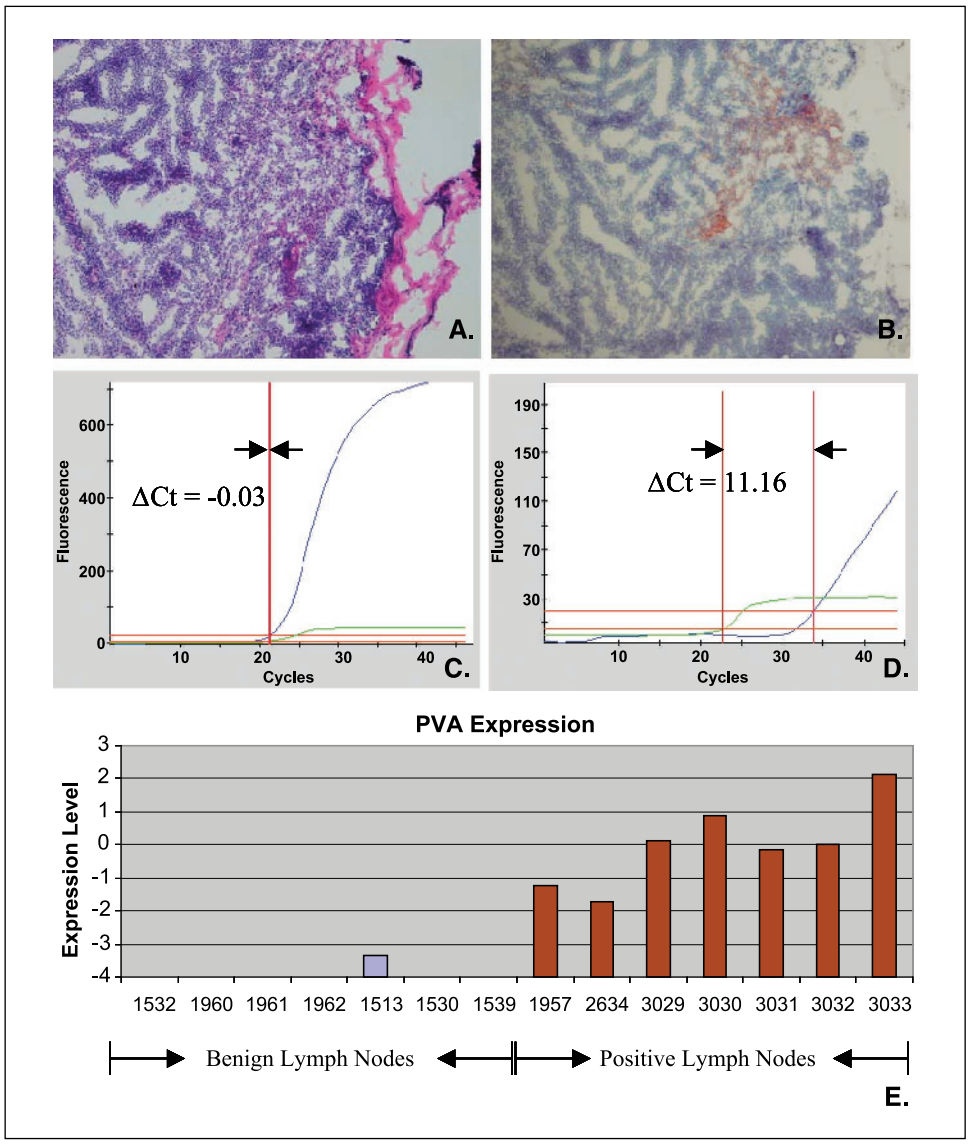

Figure 3. *PVA* expression in benign nodes and head and neck cancer positive lymph nodes as measured on GeneXpert. *A,* H&E staining of sample 2,634; *B,* immunohistochemistry staining of same area in sample 2,634; *C,* amplification plot of positive node sample 3,032 (positive in QRT-PCR); *D,* amplification plot of benign node sample 1,513 (negative in QRT-PCR); *E,* expression of 14 lymph nodes from individual patients.

likely to exist if SLN biopsy is done for this tumor type (21). This is a particularly undesirable scenario in SCCHN and could significantly reduce the acceptance of SLN biopsy by head and neck cancer surgeons.

We and others have previously shown that RT-PCR can potentially be more sensitive than routine pathology for analysis of lymph nodes (7, 26, 28). In head and neck cancer specifically, studies on molecular analysis of cervical lymph node metastasis have used a variety of techniques, including PCR amplification to detect *p53* mutations (45), immunohistochemistry staining (with or without serial sectioning) and histopathologic examination (14–16), and standard RT-PCR–based analysis of tumor maker gene expression (46). More recently, several groups have used quantitative RT-PCR for detection of cervical lymph node metastases (8, 47) and Nieuwenhuis et al. showed the prognostic value of QRT-PCR in pN0 SCCHN patients (33). This same group also showed the potential for molecular staging of cervical nodes by using tissue obtained via fine-needle aspiration (29). Despite this encouraging work, however, issues remain regarding the most appropriate molecular marker for SCCHN lymph node analysis and the reproducibility and quality control of QRT-PCR in a clinical setting. Furthermore, no studies have thus far addressed the possibility for intraoperative QRT-PCR analysis of cervical lymph nodes in patients with SCCHN. We address all of these issues in this report.

First, we have done a comprehensive marker screen to identify the best mRNA markers for detection of lymph node metastases in SCCHN. This marker screen has identified four (*SCCA1/2*, *PVA*, *TACSTD1*, and *PTHrP*) extremely robust, tumor-related markers, any one of which might be used in a single-marker assay. Squamous cell carcinoma antigen (SCCA) is a member of the ovalbumin family of serine proteinase inhibitors. The SCCA protein is expressed in neutral and acidic forms, designated as *SCCA1* and *SCCA2*, and is detected in the superficial and intermediate layers of normal squamous epithelium. The expression of *SCCA2* in cancer has been associated with an aggressive phenotype and this gene has been used in several studies for detection of squamous cell carcinoma metastases to lymph nodes (48). *TACSTD1*, also known as EPCAM, EGP-2, KS1/4, GA-733-2, and MIC-18, is a human cell surface antigen that is defined by the monoclonal antibody AUAI. *TACSTD1* is also the antigen for the antibody Ber-Ep4 and as such has been used in

studies to detect lymph node micrometastases in a variety of tumor types, including SCCHN (41, 49, 50). A recent study has also shown that *TACSTD1* is a good marker for RT-PCR–based identification of lymph node micrometastasis in non–small cell lung cancer (9). Parathyroid hormone–related protein (PTHrP, also known as PTHLH and HHM) regulates endochondral bone development and epithelial-mesenchymal interactions during the formation of the mammary glands and teeth, and its expression in SCCHN may represent dedifferentiation commonly seen in epithelial tumors. The gene encoding PTHrP has been mapped to the short arm of chromosome 12 and is known to contain 6 to 7 exons. Alternate RNA splicing of this gene results in heterogeneity of the mRNA species encoded at the 3′ ends. Pemphigus vulgaris antigen (PVA), also known as desmoglein 3 (DSG-3), is a 130-kDa surface glycoprotein that is the serologic target in the autoimmune skin disease pemphigus vulgaris. *PVA* is a member of the desmoglein subfamily of the desmosomal cadherins and the gene encoding this protein has been mapped to the long arm of chromosome 18 and is known to contain 15 exons. To our knowledge, neither *PTHrP* nor *PVA* have been used in prior studies to detect lymph node metastases in SCCHN or other tumor types.

From our data it is clear that *PVA* and *TACSTD1* are the best individual markers studied. In all screening phases, *PVA* and *TACSTD1* provided 100% discrimination between positive and benign lymph nodes although *PVA* was the only individual marker to maintain 100% classification accuracy upon bootstrap analysis. Thus, it seems that a single marker QRT-PCR analysis for *PVA* could be adequate for staging of cervical lymph nodes in SCCHN.

Whereas the marker screening phase of this study was done using routine QRT-PCR techniques, we have previously published work showing that it is possible to perform QRT-PCR assays in an intraoperative time frame (~25 minutes; refs. 34, 35). Given the potential utility of an intraoperative SLN analysis in SCCHN, we therefore applied our rapid, multiplex QRT-PCR techniques to develop such an assay for *PVA*. This assay was incorporated into a completely automated RNA isolation and QRT-PCR instrument (the GeneXpert) developed by Cepheid for molecular diagnostic testing. The GeneXpert is an automated cartridge processor with integrated real-time PCR capability. Each single-use GeneXpert cartridge consists of multiple reagent reservoirs, a syringe barrel, and a valve mechanism that allows transfer of reagents between reservoirs. In addition, the cartridges used in this study have a solid-phase matrix for nucleic acid purification and isolation. Finally, each cartridge has a PCR tube that can be accessed from specific reagent reservoirs to allow loading of reaction components into the PCR tube for reverse transcription and/or quantitative PCR. The GeneXpert instrument itself interfaces with the cartridge to control reagent movement and also houses heat plates and optical excite/detect blocks to facilitate real-time PCR. The details of RNA isolation and QRT-PCR using the GeneXpert are to be published elsewhere.

Although the speed of the GeneXpert allows for intraoperative analysis of SLNs there may also be additional clinical value if QRT-PCR eventually proves superior to routine pathology, as suggested by Nieuwenhuis et al. (33). The detection of occult lymph node disease, and subsequent improved patient staging (28), could have significant consequences for the treatment of SCCHN. For example, patients with multiple positive nodes, or extracapsular extension of tumor, are often referred for radiation or chemoradiation therapy, to reduce the high risk of locoregional failure. Although QRT-PCR cannot distinguish extracapsular extension, it may well identify additional positive lymph nodes leading to upstaging, and more appropriate adjuvant treatment. Furthermore, surgical approach and extent of lymph node dissection may also be determined by the lymph node status. Many surgeons advocate planned lymph node dissection in N2 patients who undergo primary chemoradiation because the available data indicate that 20% to 30% of complete responders (based on clinical modalities) may actually have residual tumor in the neck (3). Evaluation of suspicious postradiation cervical nodules could potentially be done via fine-needle aspirate and QRT-PCR, or by intraoperative QRT-PCR, allowing the surgeon to determine the necessary extent of resection before or during the surgery. Thus, the detection of occult lymph node metastasis could play an important role in future staging and treatment options for pathologically node-positive as well as node-negative patients.

In conclusion, we have showed that QRT-PCR can detect, with high sensitivity and specificity, metastatic disease in lymph nodes of patients with SCCHN. In addition, we have showed the feasibility of automated, intraoperative staging of cervical lymph nodes and the possibility that such an approach may eventually prove superior to conventional pathology. Staging of the cN0 neck is currently a topic of intense interest in the head and neck oncologic community, with the goal that therapeutic surgical and adjuvant treatment be administered to those most likely to benefit from it. Whereas the ACOSOG Z0360 trial is powered to validate the multiple single-institution studies that suggest the utility of SLN mapping for staging the cN0 neck in SCCHN, it is unlikely that SLN biopsy will be widely accepted without a rapid, accurate, and standardized method of staging the SLN(s). Our development of such an assay and identification of discriminatory marker genes provides the pilot data necessary for the incorporation of QRT-PCR into future clinical studies applying SLN mapping to clinical practice for patients with this disease.

Acknowledgments

Received 10/19/2004; revised 12/14/2004; accepted 1/6/2005.

Grant support: NIH/National Cancer Institute CA90665-01 research grant (T.E. Godfrey), University of Pittsburgh Oral Cancer Center of Discovery pilot grant (R.L. Ferris and T.E. Godfrey), and a cooperative research and development agreement with Cepheid (T.E. Godfrey).

The costs of publication of this article were defrayed in part by the payment of page charges. This article must therefore be hereby marked *advertisement* in accordance with 18 U.S.C. Section 1734 solely to indicate this fact.

References

1. Thekdi AA, Ferris RL. Diagnostic assessment of laryngeal cancer. Otolaryngol Clin North Am 2002;35:953–69.
2. Takes RP. Staging of the neck in patients with head and neck squamous cell cancer: imaging techniques and biomarkers. Oral Oncol 2004;40:656–67.
3. Ferlito A, Rinaldo A, Devaney KO, et al. Prognostic significance of microscopic and macroscopic extracapsular spread from metastatic tumor in the cervical lymph nodes. Oral Oncol 2002;38:747–51.
4. Curtin HD, Ishwaran H, Mancuso AA, Dalley RW, Caudry DJ, McNeil BJ. Comparison of CT and MR imaging in staging of neck metastases. Radiology 1998;207:123–30.
5. Hyde NC, Prvulovich E, Newman L, Waddington WA, Visvikis D, Ell P. A new approach to pre-treatment assessment of the N0 neck in oral squamous cell carcinoma: the role of sentinel node biopsy and positron emission tomography. Oral Oncol 2003;39:350–60.
6. Duvvuri U, Simental AA Jr, Johnson JT, et al. Elective neck dissection and survival in patients with squamous

cell carcinoma of the oral cavity and oropharynx. Laryngoscope 2004;114:2228–34.
7. Liefers GJ, Cleton-Jansen AM, van de Velde CJ, et al. Micrometastases and survival in stage II colorectal cancer. N Engl J Med 1998;339:223–8.
8. Onishi A, Nakashiro K, Mihara M, et al. Basic and clinical studies on quantitative analysis of lymph node micrometastasis in oral cancer. Oncol Rep 2004;11:33–9.
9. Mitas M, Cole DJ, Hoover L, et al. Real-time reverse transcription-PCR detects KS1/4 mRNA in mediastinal lymph nodes from patients with non-small cell lung cancer. Clin Chem 2003;49:312–5.
10. McGuirt WF, Johnson JT, Myers EN, Rothfield R, Wagner R. Floor of mouth carcinoma. The management of the clinically negative neck. Arch Otolaryngol Head Neck Surg 1995;121:278–82.
11. Alvi A, Johnson JT. Extracapsular spread in the clinically negative neck (N0): implications and outcome. Otolaryngol Head Neck Surg 1996;114:65–70.
12. Pitman KT, Johnson JT, Myers EN. Effectiveness of selective neck dissection for management of the clinically negative neck. Arch Otolaryngol Head Neck Surg 1997;123:917–22.
13. Greenberg JS, el Naggar AK, Mo V, Roberts D, Myers JN. Disparity in pathologic and clinical lymph node staging in oral tongue carcinoma. Implication for therapeutic decision making. Cancer 2003;98:508–15.
14. Ambrosch P, Brinck U. Detection of nodal micrometastases in head and neck cancer by serial sectioning and immunostaining. Oncology (Huntingt) 1996;10:1221–6.
15. Enepekides DJ, Sultanem K, Nguyen C, Shenouda G, Black MJ, Rochon L. Occult cervical metastases: immunoperoxidase analysis of the pathologically negative neck. Otolaryngol Head Neck Surg 1999;120:713–7.
16. Kocaturk S, Yilmazer D, Onal B, Erkam U, Urunal B. Do micrometastases detected with cytokeratin immunoperoxidase reactivity affect the treatment approach to neck in supraglottic cancers? Otolaryngol Head Neck Surg 2003;128:407–11.
17. Shoaib T, Soutar DS, MacDonald DG, et al. The accuracy of head and neck carcinoma sentinel lymph node biopsy in the clinically N0 neck. Cancer 2001;91:2077–83.
18. Rassekh CH, Johnson JT, Myers EN. Accuracy of intraoperative staging of the NO neck in squamous cell carcinoma. Laryngoscope 1995;105:1334–6.
19. Koch WM, Choti MA, Civelek AC, Eisele DW, Saunders JR. γ Probe-directed biopsy of the sentinel node in oral squamous cell carcinoma. Arch Otolaryngol Head Neck Surg 1998;124:455–9.
20. Zitsch RP III, Todd DW, Renner GJ, Singh A. Intraoperative radiolymphoscintigraphy for detection of occult nodal metastasis in patients with head and neck squamous cell carcinoma. Otolaryngol Head Neck Surg 2000;122:662–6.
21. Civantos FJ, Gomez C, Duque C, et al. Sentinel node biopsy in oral cavity cancer: correlation with PET scan and immunohistochemistry. Head Neck 2003;25:1–9.
22. Chao C, Wong SL, Ackermann D, et al. Utility of intraoperative frozen section analysis of sentinel lymph nodes in breast cancer. Am J Surg 2001;182:609–15.
23. Gulec SA, Su J, O'Leary JP, Stolier A. Clinical utility of frozen section in sentinel node biopsy in breast cancer. Am Surg 2001;67:529–32.
24. Tanis PJ, Boom RP, Koops HS, et al. Frozen section investigation of the sentinel node in malignant melanoma and breast cancer. Ann Surg Oncol 2001;8:222–6.
25. Koopal SA, Tiebosch AT, Albertus PD, Plukker JT, Schraffordt KH, Hoekstra HJ. Frozen section analysis of sentinel lymph nodes in melanoma patients. Cancer 2000;89:1720–5.
26. Godfrey TE, Raja S, Finkelstein SD, Gooding WE, Kelly LA, Luketich JD. Prognostic value of quantitative reverse transcription-polymerase chain reaction in lymph node-negative esophageal cancer patients. Clin Cancer Res 2001;7:4041–8.
27. Shivers SC, Wang X, Li W, et al. Molecular staging of malignant melanoma: correlation with clinical outcome. JAMA 1998;280:1410–5.
28. Bostick PJ, Morton DL, Turner RR, et al. Prognostic significance of occult metastases detected by sentinel lymphadenectomy and reverse transcriptase-polymerase chain reaction in early-stage melanoma patients. J Clin Oncol 1999;17:3238–44.
29. Nieuwenhuis EJ, Jaspars LH, Castelijns JA, et al. Quantitative molecular detection of minimal residual head and neck cancer in lymph node aspirates. Clin Cancer Res 2003;9:755–61.
30. Zehentner BK, Dillon DC, Jiang Y, et al. Application of a multigene reverse transcription-PCR assay for detection of mammaglobin and complementary transcribed genes in breast cancer lymph nodes. Clin Chem 2002;48:1225–31.
31. Xi L, Luketich JD, Raja S, et al. Molecular staging of lymph nodes from patients with esophageal adenocarcinoma. Clin Cancer Res. In press 2005.
32. Mitas M, Mikhitarian K, Walters C, et al. Quantitative real-time RT-PCR detection of breast cancer micrometastasis using a multigene marker panel. Int J Cancer 2001;93:162–71.
33. Nieuwenhuis EJ, Leemans CR, Kummer JA, et al. Assessment and clinical significance of micrometastases in lymph nodes of head and neck cancer patients detected by E48 (Ly-6D) quantitative reverse transcription-polymerase chain reaction. Lab Invest 2003;83:1233–40.
34. Raja S, El Hefnawy T, Kelly LA, Chestney ML, Luketich JD, Godfrey TE. Temperature-controlled primer limit for multiplexing of rapid, quantitative reverse transcription-PCR assays: application to intraoperative cancer diagnostics. Clin Chem 2002;48:1329–37.
35. Raja S, Luketich JD, Kelly LA, Gooding WE, Finkelstein SD, Godfrey TE. Rapid, quantitative reverse transcriptase-polymerase chain reaction: Application to intraoperative molecular detection of occult metastases in esophageal cancer. J Thorac Cardiovasc Surg 2002;123:475–83.
36. Godfrey TE, Kim S-H, Chavira M, et al. Quantitative mRNA expression analysis from formalin-fixed, paraffin-embedded tissues using 5′ nuclease quantitative RT-PCR. J Mol Diagn 2000;2:84–91.
37. Tassone F, Hagerman RJ, Taylor AK, Gane LW, Godfrey TE, Hagerman PJ. Elevated levels of FMR1 mRNA in carrier males: a new mechanism of involvement in the fragile-X syndrome. Am J Hum Genet 2000;66:6–15.
38. Morrison TB, Weis JJ, Wittwer CT. Quantification of low-copy transcripts by continuous SYBR Green I monitoring during amplification. Biotechniques 1998;24:954–8, 960, 962.
39. Efron B, Tibshirani RJ. An introduction to the bootstrap. Hardcover ed. Boca Raton: Chapman & Hall/CRC; 1994.
40. Takes RP, Baatenburg de Jong RJ, Schuuring E, et al. Markers for assessment of nodal metastasis in laryngeal carcinoma. Arch Otolaryngol Head Neck Surg 1997;123:412–9.
41. Takes RP, Baatenburg de Jong RJ, Wijffels K, et al. Expression of genetic markers in lymph node metastases compared with their primary tumours in head and neck cancer. J Pathol 2001;194:298–302.
42. Zeng Q, Smith DC, Suscovich TJ, Gooding WE, Trump DL, Grandis JR. Determination of intermediate biomarker expression levels by quantitative reverse transcription-polymerase chain reaction in oral mucosa of cancer patients treated with liarozole. Clin Cancer Res 2000;6:2245–51.
43. Turner RR, Ollila DW, Krasne DL, Giuliano AE. Histopathologic validation of the sentinel lymph node hypothesis for breast carcinoma. Ann Surg 1997;226:271–6.
44. Cote RJ, Peterson HF, Chaiwun B, et al. Role of immunohistochemical detection of lymph-node metastases in management of breast cancer. International Breast Cancer Study Group. Lancet 1999;354:896–900.
45. Brennan JA, Mao L, Hruban RH, et al. Molecular assessment of histopathological staging in squamous-cell carcinoma of the head and neck. N Engl J Med 1995;332:429–35.
46. Hamakawa H, Fukizumi M, Bao Y, et al. Genetic diagnosis of micrometastasis based on SCC antigen mRNA in cervical lymph nodes of head and neck cancer. Clin Exp Metastasis 1999;17:593–9.
47. Becker MT, Shores CG, Yu KK, Yarbrough WG. Molecular assay to detect metastatic head and neck squamous cell carcinoma. Arch Otolaryngol Head Neck Surg 2004;130:21–7.
48. Kano M, Shimada Y, Kaganoi J, et al. Detection of lymph node metastasis of oesophageal cancer by RT-nested PCR for SCC antigen gene mRNA. Br J Cancer 2000;82:429–35.
49. Kubuschok B, Passlick B, Izbicki JR, Thetter O, Pantel K. Disseminated tumor cells in lymph nodes as a determinant for survival in surgically resected non-small-cell lung cancer. J Clin Oncol 1999;17:19–24.
50. Schroder CP, Ruiters MH, de Jong S, et al. Detection of micrometastatic breast cancer by means of real time quantitative RT-PCR and immunostaining in perioperative blood samples and sentinel nodes. Int J Cancer 2003;106:611–8.

Molecular Staging of Cervical Lymph Nodes in Squamous Cell Carcinoma of the Head and Neck

Robert L. Ferris, Liqiang Xi, Siva Raja, et al.

Cancer Res 2005;65:2147-2156.